20th Australasian Fluid Mechanics Conference
Perth, Australia
5-8 December 2016

The Structure of Turbulence Across the Sediment-Water-Interface

J. Voermans[1], M. Ghisalberti[1,2] and G. N. Ivey[1,3]

[1]School of Civil, Environmental and Mining Engineering
University of Western Australia, Crawley, Western Australia 6009, Australia

[2]Department of Infrastructure Engineering
University of Melbourne, Parkville, Victoria, 3010, Australia

[3]The UWA Oceans Institute
University of Western Australia, Crawley, Western Australia, 6009, Australia

Abstract

An increasing body of literature indicates that turbulence is a major contributor to the exchange of mass and momentum across the sediment-water-interface (SWI). The permeability Reynolds number $Re_K = \sqrt{K}u_*/\upsilon$ is a key parameter describing the flow at the SWI, where K is the permeability of the porous medium. The dynamics of turbulence around the SWI are determined by the intricate interaction between the hydrodynamics and the sediment characteristics, however, traditional experimental techniques are hindered in accessing this region properly, making experimental data rare. In this work we describe novel experimental results, which combines refractive index matching (RIM) and particle tracking velocimetry (PTV), and capture the instantaneous velocity fields across the SWI, for two different values of Re_K. The measurements enable us to evaluate the TKE budget, a key tool for understanding turbulent processes. The results show that for low Re_K the TKE-budget is in good agreement with DNS results for an impermeable boundary. For the same permeability but larger Re_K, the flow penetrates the interface and the TKE-budget shows turbulence is both produced and transported beyond the SWI and into the permeable medium. Unlike the low Re_K case where at the interface only viscous diffusion and dissipation are dominant, in the high Re_K case all terms in the TKE-budget are of importance.

Introduction

An important issue for environmental management is the transport processes at the sediment-water-interface (SWI) and the contribution of turbulence to the transfer of properties across the interface. While the small turbulent length and velocity scales near a low porosity boundary (such as the SWI) suggest that viscous and molecular forces dominate mass and momentum transfer (e.g. [1]), experimental measurements indicate significant higher fluxes than can be explained by laminar effects alone [4, 8]. The discrepancies are generally attributed to either the indirect [5, 7] or the direct influence of turbulence at the interface [8, 12]. The enhancement of interfacial fluxes show a strong correlation with the permeability Reynolds number $Re_K = \sqrt{K}u_*/\upsilon$, suggesting the boundary acts as an impermeable interface for $Re_K \ll 1$ in which turbulence can enhance the transfer of properties indirectly by modifying the gradients of properties above the interface. For $Re_K \gg 1$ the interface resembles a highly permeable boundary where the transport of properties across the interface are directly influenced by turbulence [14]. Little is known however about this structure of turbulence around the SWI, which has a typical $Re_K \sim O(1)$, and therefore the impact of turbulence on the solute transport and sediment transport.

The lack of understanding of the turbulent structure, is attributed to experimental limitations and specifically the technical difficulties of performing measurements close to the SWI, let alone across the interface. This makes detailed information on interfacial turbulence currently only realizable by numerical simulations. Though the simulations provide valuable data, previously considered inaccessible, the results are limited by the applied discretization methods for the sediments, which ignores the heterogeneity of a physical sediment bed. This heterogeneity can have a profound impact on the hydrodynamics across the SWI (e.g. [3, 9, 10]), and therefore also on the structure of turbulence [9].

In this paper, the structural characteristics of turbulence across the SWI are described for two values of Re_K by performing a laboratory experiment which combines refractive index matching (RIM) and particle tracking velocimetry (PTV). This unusual experimental setting allows both the replication of a physical sediment bed, and the use of non-intrusive measurement techniques, which permits detailed velocity measurements across the SWI. The structure of turbulence is examined by means of the turbulent kinetic energy (TKE) budget, as it clarifies the importance of the turbulent processes involved in interfacial transport.

Methodology

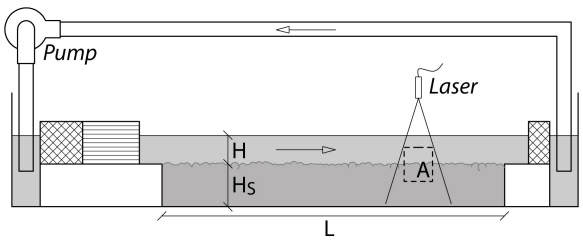

Figure 1: Experimental set-up, flow is driven by a centrifugal pump and disturbances are dampened by foam and flow straighteners. The sediment bed has a height of $H_s = 15$ cm and a length $L = 1.1$ m. The fluid depth is $H = 9$ cm, and measurements are performed in the marked area A.

The experiments were performed in a 2 m long flume in the GFD-laboratory at the University of Western Australia (see figure 1). The working fluid is a 59% sodium iodide by mass solution ($SG = 1.77$, $\upsilon = 1.35 \times 10^{-6}$ m^2/s), which has a refractive index of $n = 1.4750$, equal to that of the borosilicate glass spheres used as model for sediments. Due to the RIM, light travelling through the interstitial fluid and the sediments will not change direction, making the sediments optically invisible. The flow was seeded with silver coated PMMA partiles ($SG = 1.75$ and $d_p = 32 - 40\ \mu$m), which were continuously illuminated by

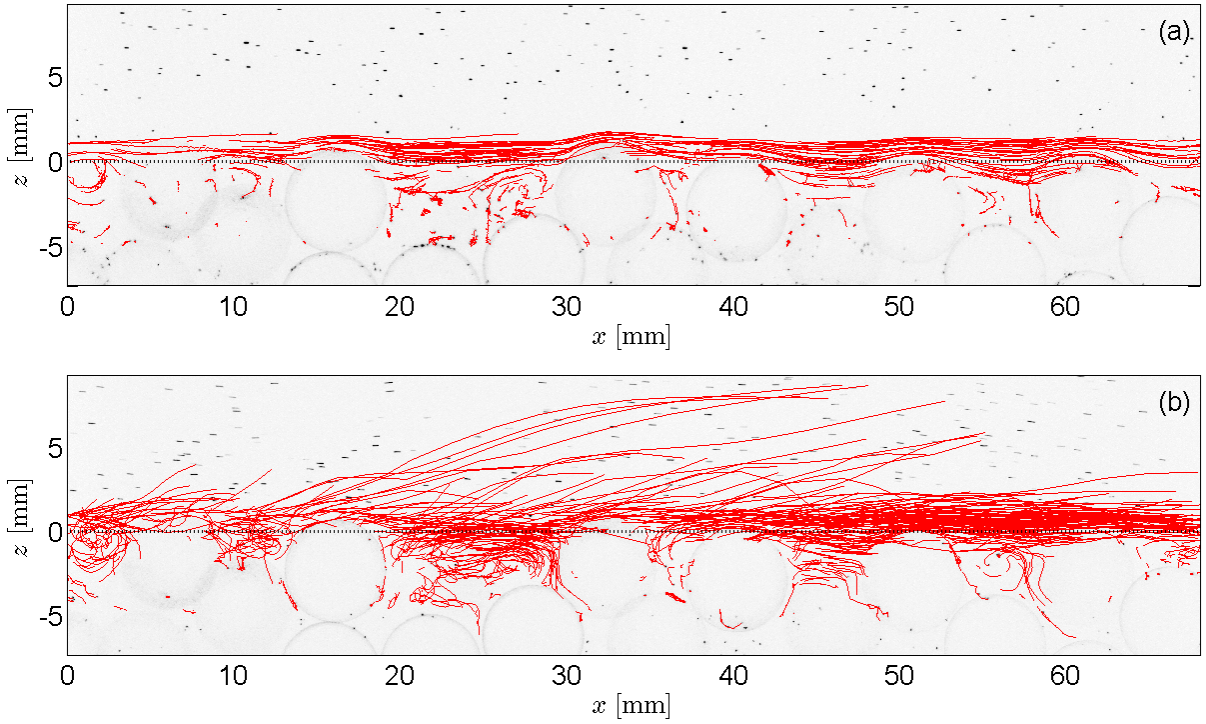

Figure 2: Particle trajectories for (a) $Re_K = 0.36$, (b) $Re_K = 0.97$. The trajectories are recorded over a time span that is inversely proportional to $U_b/\sqrt{K}$, and trajectories are highlighted only when started in between $z = [-5, 1]$ mm. In the case of $Re_K = 0.97$, particles are actively transported across the interface, which is indicated by the dashed line.

a 1 mm wide laser sheet. To create the laser sheet, two custom made 50 mW, 650 nm lasers were aligned containing a 60° fan angle Powell lens. As the reflected light of the tracer particles is undistorted by the presence of the sediment bed, the local positions of the particles can be captured by a camera across the SWI. The frames were recorded at a rate of 23 fps, covering a region of 35×70 mm (*A* in figure 1), at three lateral positions. The captured images were post-processed in the PTV-system *Streams*, a system regularly applied to the experimental study of turbulent boundary flows, e.g. [11]. The diameter of the borosilicate glass spheres is $d = 6$ mm, creating a monodisperse sediment bed with a permeability of $K = 3.96 \times 10^{-2}$ mm^2, determined through the Karman-Cozeny relation. The two experimental cases examined have a bulk velocity U_b of 31 and 82 mm/s respectively, and Re_K values of 0.36 and 0.97. Note that, hereafter, properties of each case are indicated by the subscripts $_{c36}$ and $_{c97}$ respectively. The shear velocity u_* is defined as $u_* = \sqrt{\tau_{max}/\rho}$, where τ_{max} is the maximum spatial-averaged shear stress in the vertical profile. The vertical porosity profile $\theta(z)$ can be obtained from the recorded images and is used to define the position of the interface, defined as the inflection point of the porosity profile. Uncertainties in the porosity profile were estimated to be less than 2%.

Particle Trajectories

The difference between a permeable and impermeable SWI is illustrated in figure 2, where the trajectories of tracer particles in a fixed time frame are shown starting between $z = [-5, 1]$ mm. For $Re_K = 0.36$, the boundary acts as a near-impermeable interface, where particles mainly disperse due to the obstruction of the individual elements, but do not actively reach the interstitial fluid by penetrating the interface. Though some exchange seems to exist, the main flow in the pore space is re-circulation only. The trajectories for $Re_K = 0.97$ in the same region are, however, much more variable, and, unlike at $Re_K = 0.36$, are not dictated by the contours of the sediment bed (see figure 2a). In between the individual grains, particles are not just forming a recirculation zone, the particles tend to move periodically back and forward, presumably due to turbulence-induced pressure disturbances above the sediment bed.

The particle trajectories of the two cases clearly demonstrate the influence of Re_K on transport processes across the SWI, as the absolute permeability K is equal in both cases. It is in particular the frequency at which particles are ejected into the fluid column from the interstitial fluid (i.e. see figure 2b), that is suggestive of enhanced interfacial transport at higher Re_K.

TKE-budget

The dynamics of turbulence at the SWI can be elucidated by examining the TKE-budget. As the measurements only provide information on the velocity in two directions, namely the streamwise and wall-normal direction (x and z respectively), not all components of the TKE-equations can be measured. However, assuming that the flow can be approximated as being two-dimensional and fully developed, it can be concluded that the major energy containing components can be determined [9]. The production of TKE (P) and the turbulent transport of TKE (TT) are given by

$$P = -\overline{u_i' u_j'} \frac{\partial \overline{u}_i}{\partial x_j} \tag{1}$$

$$TT = -\frac{1}{2} \frac{\partial \overline{u_i' u_i' u_j'}}{\partial x_j} \tag{2}$$

where for both P and TT four components can be determined, for i and $j = 1, 3$. The spatial variation of P and TT for $Re_K = 0.36$ shows great similarities with that of an impermeable boundary, where TKE is produced in the near-wall region

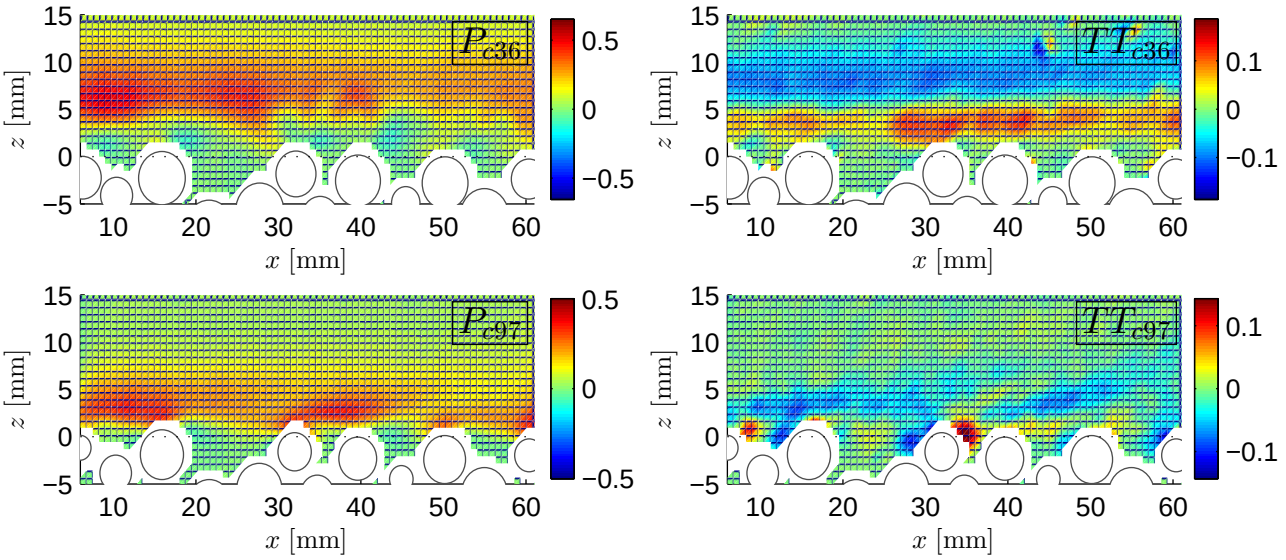

Figure 3: TKE production and turbulent transport for $Re_K = 0.36$ and $Re_K = 0.97$ respectively, normalized by u_*^4/υ. The TKE is produced primarily above the boundary, and transported towards the interface for $Re_K = 0.36$, and across the interface for $Re_K = 0.97$.

(see figure 3, P_{c36}). The components seem to be nearly unaffected by the presence of the individual sediment elements, as the high and low energy peaks present itself in nearly continuous horizontal bands. The same components but for $Re_K = 0.97$ are also shown in figure 3, revealing the region of TKE production to be closer to the interface and also a higher degree of heterogeneity compared to $Re_K = 0.36$. The local production of TKE suggest small shear layers originating from individual roughness elements (see figure 3, TT_{c97}). These local shear layers correspond to the transport of TKE into the pore spaces of the roughness elements, which substantiates the observation in figures 2 that turbulence plays an active role in mass transport across the interface for higher Re_K.

The spatial variation of P and TT demonstrate the sensitivity of the hydrodynamics to the local irregularity of the boundary, at least for increasing Re_K. Consequently, to assess the details of the turbulent processes from a macroscopic point of view, spatial averaging is a necessity. The procedure, also known as double-averaging (DA) in both time and space, follows the Reynolds-decomposition ($\xi = \overline{\xi} + \xi'$) with a spatial decomposition, given by $\overline{\xi} = \left\langle \overline{\xi} \right\rangle + \widetilde{\xi}$ (e.g. [10]). The DA-TKE equation, as in [9, 13], is then given by

$$
\begin{aligned}
0 \quad = \quad & \underbrace{-\theta(z)\left\langle \overline{u_i' u_j'} \right\rangle \frac{\partial \langle \overline{u}_i \rangle}{\partial x_j}}_{(1)} \underbrace{-\theta(z)\left\langle \widetilde{u_i' u_j'} \frac{\partial \widetilde{u}_i}{\partial x_j} \right\rangle}_{(2)} \\
& \underbrace{-\frac{1}{2}\frac{\partial\, \theta(z)\left\langle \overline{u_i' u_i' u_j'} \right\rangle}{\partial x_j}}_{(3)} \underbrace{-\frac{1}{2}\frac{\partial\, \theta(z)\left\langle \widetilde{u_i' u_i'} \widetilde{u_j} \right\rangle}{\partial x_j}}_{(4)} \\
& \underbrace{-\frac{1}{\rho}\frac{\partial\, \theta(z)\left\langle \overline{p' u_j'} \right\rangle}{\partial x_j}}_{(5)} \underbrace{+\theta(z)\upsilon \frac{\partial^2 \left\langle \overline{u_i'^2} \right\rangle}{\partial x_j^2}}_{(6)} \\
& \underbrace{-\theta(z)\upsilon \left\langle \overline{\left(\frac{\partial u_i'}{\partial x_j} \right)^2} \right\rangle}_{(7)}
\end{aligned}
\tag{3}
$$

where terms one and two represent the production of TKE, the third and fourth terms the transport of TKE by turbulence, the fifth and sixth terms the redistribution of TKE by pressure fluctuations and viscosity respectively, and the seventh term the dissipation of TKE. Note that terms 2 and 4 are additional terms originating from the spatial averaging procedure, and are generated by spatial velocity correlations. The fifth term and all components related to the lateral direction, i.e. $i = 2$ and/or $j = 2$, are grouped in a residual term. The uncertainty in our measured budget terms is dominated by the spatial variability of the porous medium and is estimated by evaluating the influence of each measurement on the spatial average values. The turbulent transport term is found to be most variable, estimated to cause an uncertainty limited to 30%. The differences between the two Re_K cases examined, however, greatly exceeds this uncertainty.

As the $Re_K = 0.36$ reveals flow characteristics similar to that of an impermeable boundary, the DA-TKE profiles are compared to that from DNS results of a turbulent boundary layer over a flat plate [6]. The SWI results show good agreement with the DNS results (see figure 4a), with maxima of the various components of similar magnitude and occurring at similar vertical positions. Contrary to the TKE-budget of $Re_K = 0.36$, where at the interface viscous diffusion and dissipation of TKE dominate, all processes are relevant at the SWI for $Re_K = 0.97$. Beyond the interface, the dissipation seems to balance the turbulent transport and the viscous diffusion terms (figure 4b). The residual term is of the same order as the dissipation term, which likely contains energy from the dissipation term as this term is not fully resolved. However, others have related this term also to the importance of the redistribution of TKE by pressure fluctuations [2].

Conclusions

The structure of turbulence across the SWI is experimentally examined for two cases of Re_K by means of the TKE-budget, revealing the direct contribution of turbulence on interfacial transport. While for low Re_K boundaries viscous diffusion and dissipation of TKE dominate at the SWI, resembling an impermeable boundary, increasing Re_K reveals all processes in the TKE-budget to be of importance at the interface. This differ-

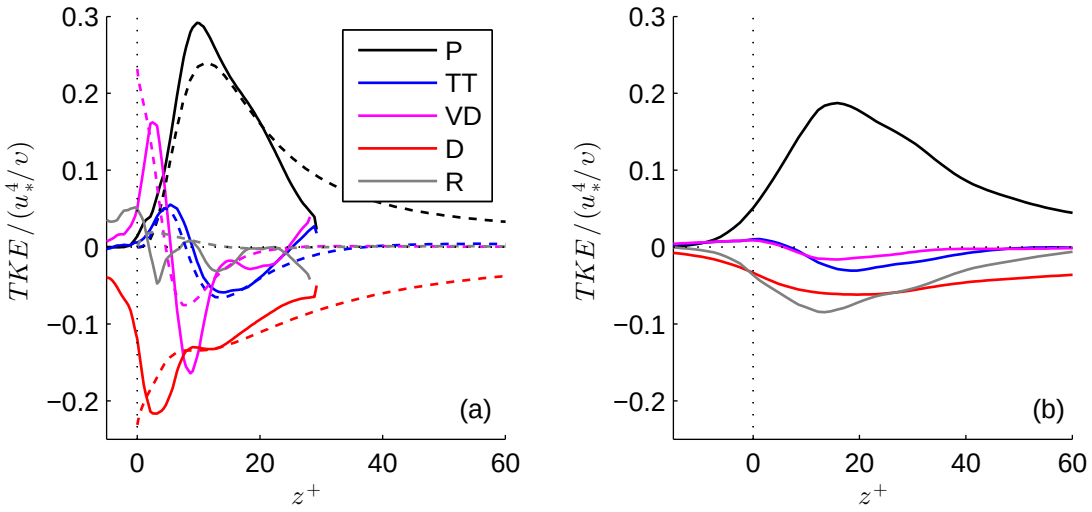

Figure 4: DA-TKE budget for (a) $Re_K = 0.36$, (b) $Re_K = 0.97$; with TKE production P, turbulent transport TT, viscous diffusion VD, dissipation D and the residual R. The dashed lines correspond to the TKE budget for the impermeable boundary obtained from DNS [6]. The TKE budget is normalized by u_*^4/υ and the vertical coordinate z is presented in viscous wall units. While for $Re_K = 0.36$ the budget at the interface reduces to an equilibrium between D and VD, for $Re_K = 0.97$, all terms become of importance.

ence has significant dynamic implications for future research in fields such as benthic hydrodynamics and sediment transport.

Acknowledgements

This research was supported under Australian Research Council's *Discovery Projects* funding scheme (project number DP120102500).

References

[1] Boudreau, B. P., *Solute transport above the sediment-water interface*, Oxford Univ. Press New York, 2001.

[2] Breugem, W. P., Boersma, B. J. and Uittenbogaard, R. E., The influence of wall permeability on turbulent channel flow, *Journal of Fluid Mechanics*, **562**, 2006, 35–72.

[3] Goyeau, B., Lhuillier, D., Gobin, D. and Velarde, M. G., Momentum transport at a fluidporous interface, *International Journal of Heat and Mass Transfer*, **46**, 2003, 4071–4081.

[4] Grant, S. B., Stewardson, M. J. and Marusic, I., Effective diffusivity and mass flux across the sediment-water interface in streams, *Water Resources Research*, **48**.

[5] Hondzo, M., Feyaerts, T., Donovan, R. and O'Connor, B. L., Universal scaling of dissolved oxygen distribution at the sediment-water interface: A power law, *Limnology and oceanography*, **50**, 2005, 1667–1676.

[6] Kim, J., Moin, P. and Moser, R., Turbulence statistics in fully developed channel flow at low reynolds number, *Journal of Fluid Mechanics*, **177**, 1987, 133–166.

[7] Lorke, A., Muller, B., Maerki, M. and Wuest, A., Breathing sediments: The control of diffusive transport across the sediment-water interface by periodic boundary-layer turbulence, *Limnology and Oceanography*, **48**, 2003, 2077–2085.

[8] Manes, C., Ridolfi, L. and Katul, G., A phenomenological model to describe turbulent friction in permeable-wall flows, *Geophysical Research Letters*, **39**.

[9] Mignot, E., Barthelemy, E. and Hurther, D., Double-averaging analysis and local flow characterization of near-bed turbulence in gravel-bed channel flows, *Journal of Fluid Mechanics*, **618**, 2009, 279–303.

[10] Nikora, V., Goring, D., McEwan, I. and Griffiths, G., Spatially averaged open-channel flow over rough bed, *Journal of Hydraulic Engineering*, **127**, 2001, 123–133.

[11] Nikora, V., Nokes, R., Veale, W., Davidson, M. and Jirka, G., Large-scale turbulent structure of uniform shallow free-surface flows, *Environmental Fluid Mechanics*, **7**, 2007, 159–172.

[12] Packman, A. I., Salehin, M. and Zaramella, M., Hyporheic exchange with gravel beds: Basic hydrodynamic interactions and bedform-induced advective flows, *Journal of Hydraulic Engineering*, **130**, 2004, 647–656.

[13] Raupach, M. and Shaw, R., Averaging procedures for flow within vegetation canopies, *Boundary-Layer Meteorology*, **22**, 1982, 79–90.

[14] Voermans, J., Ghisalberti, M. and Ivey, G., Coherent vortex structures at the sediment-water-interface, in *11th International Symposium on Ecohydraulics, Melbourne, Australia*, 2016.